Solution Structure of the Head-to-Head Dimer of Calicheamicin Oligosaccharide Domain and d(CGTAGGATATCCTACG)$_2$

Giuseppe Bifulco,[†,‡] Aldo Galeone,[‡] Luigi Gomez-Paloma,*[,§] K. C. Nicolaou,*[,§,||] and Walter J. Chazin[†]

Contribution from the Departments of Chemistry and Molecular Biology, The Scripps Research Institute, 10550 N. Torrey Pines Road, La Jolla, California 92037, Department of Chemistry, University of California at San Diego, La Jolla, California 92093, and Dipartimento di Chimica delle Sostanze Naturali, Universita' degli studi di Napoli "Federico II", via D. Montesano 49, Napoli 80131, Italy

Received May 7, 1996[⊗]

Abstract: The head-to-head dimer of the calicheamicin oligosaccharide domain exhibits an impressive nanomolar affinity for its specific DNA recognition sites and a substantially higher degree of sequence selectivity relative to the oligosaccharide monomer. In an effort to determine the structural basis for these binding properties, the solution structure of the 1:1 complex between the head-to-head dimer and the self-complementary oligonucleotide d(CGTAGGATATCCTACG)$_2$ has been solved using ^{1}H NMR-derived distance and torsion angle constraints and molecular dynamics calculations. Complete sequence specific proton assignments of both the DNA duplex and the carbohydrate have been obtained by 2D-NMR. A total of 607 experimentally derived constraints were identified including 452 proton−proton distance constraints derived from NOESY cross peaks intensities and assigned hydrogen bonds, along with 155 dihedral angle constraints obtained from a detailed analysis of the multiplet structure of cross-peaks for the sugar rings and from qualitative analysis of nuclear Overhauser effects for the DNA backbone. The final conformation of the complex is represented by an ensemble of seven structures (the average all-atom root mean square deviation from the mean is 1.07 Å in the well-defined region) obtained by refining 14 initial conformations with widely different nonstandard DNA geometries. A number of favorable interactions are found to stabilize the structure of the complex and account for binding sequence preferences. Overall, the binding mode of each oligosaccharide unit of the head-to-head dimer in the DNA minor groove seems to be very close to that observed in the case of the monomeric calicheamicin oligosaccharide bound to its corresponding TCCT recognition site. Variable temperature NMR studies have shown that this dimer binds to d(CGTAGGATATCCTACG)$_2$ in two subtly different conformations, probably differing in the positioning of rings E and E′, interconverting with a rate constant of ∼0.35 s^{-1}. The solution structure of this carbohydrate−DNA complex provides confirmation of design principles for new calicheamicin-based DNA-binding agents and confirms insights obtained previously into the molecular basis for oligosaccharide recognition within the DNA minor groove.

Introduction

Recognition is a very important phenomenon in biology and chemistry, and the molecular basis of the interaction between small ligands and biopolymers is the subject of a numerous investigations aimed at the rational design of molecules with specific biological activities.

Although there are many examples of specific interactions between organic molecules and proteins (*e.g.* substrate−enzyme interactions), few cases are known of ligands that bind duplex DNA in a sequence-specific manner. NMR spectroscopy is a useful method for the characterization of biomolecules and their complexes with small ligands.[1] Complexes of DNA with small molecule ligands such as chromomycin,[2] mithramycin,[3] distamycin,[4] and SN-6999[5] have been studied by NMR. Structural models from these studies have provided further insights into the binding phenomena and prompted the rational design of new ligands, with the ultimate goal of binding with sequence specificity to control biological activity.

The enediynes, which includes esperamicins, dynemicin A, neocarzinostatin chromophore, kedarcin chromophore, and C1027 chromophore, represent an important class of antibiotics the activity of which is associated with DNA-binding properties. Among these molecules, calicheamicin[6] (**1**, Scheme 1) displays the greatest selectivity in binding duplex DNA. Chemists and biologists have recently given calicheamicin much attention for its strong cytotoxic activity and its ability to bind and cleave DNA in a special way.[7,8] In a previous paper, we reported the solution structures of calicheamicin−DNA and of calicheamicin oligosaccharide domain−DNA complexes and showed directly that the calicheamicin oligosaccharide domain is responsible for the positioning of the enediyne moiety that cleaves the DNA duplex.[9]

[†] Department of Molecular Biology, The Scripps Research Institute.
[‡] Universitá degli studi di Napoli "Federico II".
[§] Department of Chemistry, The Scripps Research Institute.
[||] University of California at San Diego.
[⊗] Abstract published in *Advance ACS Abstracts,* September 1, 1996.

(1) Gilbert, D. E.; Feigon, J. *Curr. Opin. Struct. Biol.* **1991**, *1*, 439.
(2) Gao, X.; Mirau, P.; Patel, D. J. *J. Mol. Biol* **1992**, *223*, 259.
(3) Sastry, M.; Patel, D. J. *Biochemistry* **1993**, *32*, 6588.
(4) Dwyer, T. J.; Geierstanger, B. H.; Bathini, Y.; Lown, J. W.; Wemmer, D. E. *J. Am. Chem. Soc.* **1992**, *114*, 5911.
(5) (a) Chen, S.; Leupin, W.; Rance, M.; Chazin, W. J. *Biochemistry* **1992**, *31*, 4406. (b) Rydzewski, J.; Leupin, W.; Chazin, W. J. *Nucleic Acids Res.* **1996**, in press.
(6) (a) Nicolaou, K. C.; Dai, W.-M. *Angew. Chem. Int. Ed. Engl.* **1991**, *30*, 1387. (b) Nicolaou, K. C.; Smith, A. L.; Yue, E. W. *Proc. Natl. Acad. Sci. U.S.A.* **1993**, *90*, 5881.
(7) De Voss, J. J.; Townsend, C. A.; Ding, W. D.; Morton, G. O.; Ellestad, G. A.; Zein, N.; Tabor, A. B.; Schreiber, S. L. *J. Am. Chem. Soc.* **1990**, *112*, 9669.
(8) Hangeland, J. J.; De Voss, J. J.; Health, J. A.; Townsend, C. A.; Ding, W. D.; Ashcroft, J. S.; Ellestad, G. A. *J. Am. Chem. Soc.* **1992**, *114*, 9200.
(9) Gomez Paloma, L.; Smith, J. A.; Chazin, W. J.; Nicolaou, K. C. *J. Am. Chem. Soc.* **1994**, *116*, 3697.

S0002-7863(96)01525-9 CCC: $12.00

Scheme 1. Structures of Calicheamicin γ_1' (**1**), Calicheamicin Oligomer (**2**), and Head-to-Head Calicheamicin Oligosaccharide Dimer (**3**)

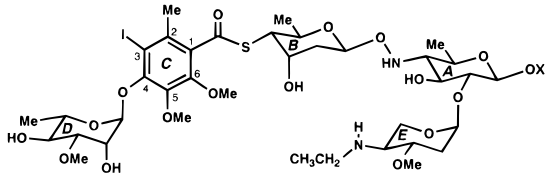

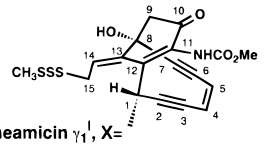

1: calicheamicin γ_1^I, X=

2: monomeric oligosaccharide, X=Me

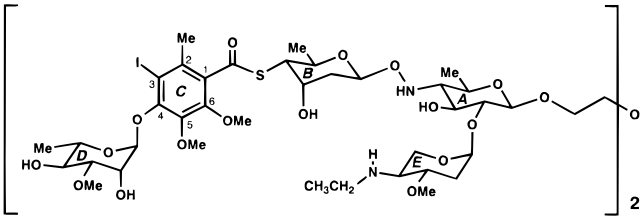

3: dimeric oligosaccharide

Recently the methyl glycoside of the calicheamicin oligosaccharide (**2**, Scheme 1) has been reported to inhibit the formation of certain transcription factor−DNA complexes in cases where the DNA recognition sequence contains a calicheamicin-binding site.[10] The observation that the binding of the methyl glycoside of the calicheamicin oligosaccharide in the minor groove blocks the association of transcription factors in the major groove supports the hypothesis that the conformation of DNA is strongly affected. These observations, together with the desire to improve the selectivity of small molecules that bind duplex DNA, suggest the need for new directions in the design and synthesis of novel carbohydrates with DNA-binding ability. Along these lines, the head-to-head dimer (HHD) of calicheamicin oligosaccharide (**3**, Scheme 1) has been designed and synthesized[11] in order to test its ability to bind a DNA sequence containing two binding sites (*e.g.* AGGA-XX-TCCT). Assuming that calicheamicin binds selectively and with approximately the same affinity to four sequences (*e.g.* TCCT, TTTT, TCTC, and ACCT),[12] the head-to-head dimer should display a theoretical specificity improvement of 64-fold with respect to calicheamicin.

Oligomers of peptidic DNA-binding agents, such as dystamicin[13] and netropsin,[14] have been synthesized and reported to recognize longer DNA sequences than their monomeric counterparts. For instance, Singh et al. have recently analyzed by NMR spectroscopy the complex of $d(CGAAAATTTTCG)_2$ and a bis-netropsin derivative.[14a] However, there are no examples of oligosaccharides capable of recognizing more than four DNA base pairs.

(10) Ho, S. N.; Boyer, S. H.; Schreiber, S. L.; Danishefsky, S. J.; Crabtree, G. R. *Proc. Natl. Acad. Sci. U.S.A.* **1994**, *91*, 9203.

(11) Nicolaou, K. C.; Ajito, K.; Komatsu, H.; Smith, B. M.; Li, T.; Egan, M. G.; Gomez Paloma, L. *Angew. Chem. Int. Ed. Engl.* **1995**, *34*, 576.

(12) (a) Zein, N.; Sinha, A. M.; McGabren, W. J.;Ellestad, G. A. *Science* **1988**, *240*, 1198. (b) Walker, S.; Landovitz, R.; Ding, W. D.; Ellestad, G. A.; Kahne, D. *Proc. Natl. Acad. Sci. U.S.A.* **1992**, *89*, 4608.

(13) (a) Youngquist, R. S. and Dervan, P. B. *J. Am. Chem.Soc.* **1985**, *107*, 5528. (b) Youngquist, R. S. and Dervan, P. B. *J. Am. Chem. Soc.* **1987**, *109*, 7564.

(14) (a) Singh, P. M.; Plouvier, B.; Hill, G. C.; Gueck, J.; Pon R. T.; Lown, J. W. *J. Am. Chem. Soc.* **1994**, *116*, 706. (b) Griffin, J. H.; Dervan, P. B. *J. Am. Chem. Soc.* **1986**, *107*, 5008.

5'-C G T A G G A T A T C C T A C G-3'
3'-G C A T C C T A T A G G A T G C-5'

Figure 1. DNA sequence used in these studies. The two recognition sites are highlighted by boxes.

Scheme 2. Protocol Used for the Structure Calculation of the HHD−DNA Complex

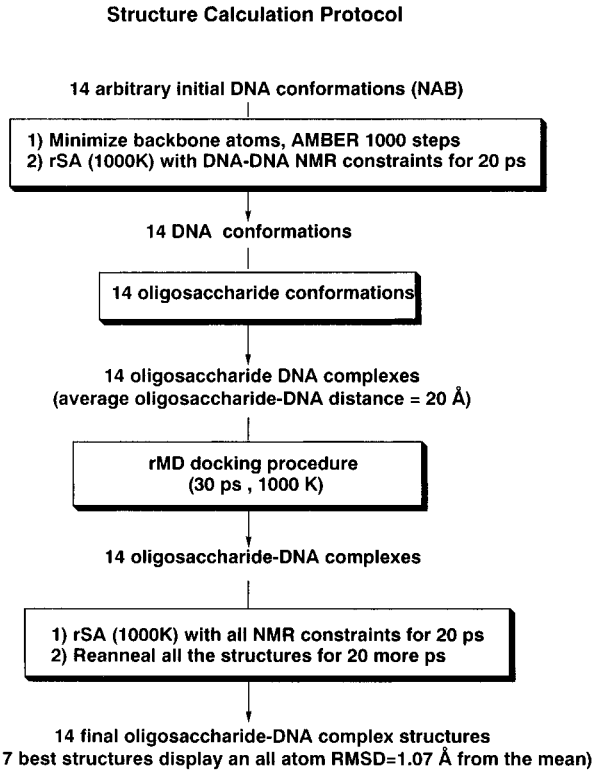

The binding of the head-to-head dimer to high-affinity duplex DNA recognition sites ($K_D = 10^{-9}$) is substantially higher than that of the oligosaccharide monomer ($K_D \sim 10^{-6}$), and it exhibits higher specificity.[15] Furthermore, binding of transcription factors to DNA, and STAT-3 dependent transcription are inhibited by compound **3**, and the activity is significantly greater than for the monomer.[16] Here we determine the solution structure of the head-to-head dimer in complex with the $d(CGTAGGATATCCTACG)_2$ palindrome (Figure 1) by NMR spectroscopy, seeking to establish if there is a structural basis for the superior binding properties and biological activity of the dimer relative to the monomer.

Experimental Section

Synthesis of the Oligonucleotide. The self-complementary 16-mer oligonucleotide d(CGTAGGATATCCTACG) was synthesized on a Beckmann 200A automatic synthesizer using phosphoramidite chemistry, purified by ion exchange HPLC on a Partisil 10 SAX column with 20% CH_3CN and a linear gradient of KH_2PO_4 from 0.01 to 0.35 M at pH 7, and then desalted by gel filtration on a Biogel P2 column.

Preparation of the Complex. The DNA strands were annealed by heating at 90 °C for 5 min, followed by slow cooling to room temperature. The NMR sample was prepared by lyophilizing the duplex twice from 99.6% D_2O and then dissolving the lyophilized material in 500 μL of 10 mM (pH 7.0) phosphate buffer containing 100 mM NaCl and 0.1 mM EDTA in 99.996% D_2O. For experiments to assign the labile protons, the sample was lyophilized and redissolved in 90% H_2O / 10% D_2O. The final concentration was 2.0 mM in duplex.

(15) Nicolaou, K. C.; Smith, B. M.; Ajito, K.; Komatsu, H.; Gomez-Paloma, L.; Tor, Y. *J. Am. Chem. Soc.* **1996**, *118*, 2303.

(16) Liu, C.; Smith, B. M.; Ajito, K.; Komatsu, H.; Gomez-Paloma, L.; Li, T.; Theodorakis, E. A.; Nicolaou, K. C.;Vogt, P. K. *Proc. Natl. Acad. Sci., U.S.A.* **1996**, *93*, 940.

Table 1. Proton Chemical Shifts in HHD−d(CGTAGGATATCCTACG)$_2$ Complex at pH 7.0, T = 300 K

DNA Chemical Shifts (ppm)[a]

residue	N_1H, N_3H	NH_2	2H, 5H, 5-Me	6H, 8H	1′H	2′H	2″H	3′H	4′H	5′H/5″H
C_1			5.89	7.61	5.76	1.99	2.40	4.67	4.05	
G_2	12.89			7.92	5.91	2.65	2.73	4.95	4.34	3.98
T_3	13.20		1.47	7.23	5.52	2.15	2.42	4.83	4.16	
A_4			7.41[b]	8.07	6.24	2.62	3.04	5.02	4.42	
G_5	12.88[c]			7.48	5.66	2.44	2.48	4.91	4.33	3.98/4.08
G_6	13.08[d]			7.68	5.38	2.42	2.72	5.03	4.34	4.16
A_7			7.66	7.96	6.27	2.41	2.94	5.04	4.41	3.12/3.33
T_8	13.52[e]		1.29	6.93	5.46	1.92	2.33	4.82	4.11	
A_9			7.40[f]	8.25	6.42	2.61	3.03	5.02	4.33	
T_{10}	13.39[g]		1.35	6.92	5.91	1.86	2.77	4.87	4.33	
C_{11}		6.40, 8.02	5.38	7.26	6.06	1.87	2.55	4.85	4.05	
C_{12}		6.63, 8.30	5.40	7.46	5.99	2.30	2.39	4.58	4.00	3.25
T_{13}	13.31[h]		1.38	7.36	5.88	1.89	2.45	4.62	4.13	
A_{14}			7.18	8.28	6.13	2.67	2.82	5.02	4.40	
C_{15}		6.46, 8.28	5.32	7.21	5.56	1.83	2.24	4.77	4.12	
G_{16}				7.87	5.49	2.33	2.56	4.58	4.15	
C_{17}			5.89	7.61	5.76	1.99	2.40	4.67	4.05	
G_{18}	12.89			7.96	5.91	2.65	2.73	4.95	4.34	3.98
T_{19}	13.20		1.47	7.26	5.52	2.15	2.42	4.84	4.16	
A_{20}			7.40[b]	8.10	6.25	2.63	2.90	5.01	4.42	
G_{21}	12.76[c]			7.46	5.66	2.36	2.75	4.93	4.33	3.98/4.08
G_{22}	12.60[d]			7.67	5.95	2.34	2.57	5.01	4.34	4.16
A_{23}			7.66	8.13	6.45	2.51	2.81	4.81	4.41	3.12/3.33
T_{24}	13.47[e]		1.09	6.88	6.05	1.84	2.54	4.73	4.29	
A_{25}			7.47[f]	8.18	6.19	2.43	2.91	4.98	4.28	
T_{26}	12.99[g]		1.24	7.05	6.04	1.94	2.66	4.84	4.16	
C_{27}		6.40, 8.02	5.43	7.32	5.77	2.05	2.40	4.68	4.05	
C_{28}		6.63, 8.30	5.40	7.46	5.99	2.30	2.39	4.58	4.00	3.25
T_{29}	13.27[h]		1.39	7.38	5.88	1.91	2.46	4.62	4.13	
A_{30}			7.18	8.31	6.22	2.69	2.88	5.01	4.40	
C_{31}		6.46, 8.28	5.37	7.26	5.64	1.83	2.24	4.88	4.14	
G_{32}				7.87	5.49	2.33	2.56	4.58	4.15	

Drug Chemical Shifts (ppm)[a]

sugar residue	H1	$H2_{ax}$	$H2_{eq}$	H3	H4	H5	Me	OMe
A	4.20	3.30		4.32	2.39	3.90	1.37	
B	5.16	1.87	2.24	4.29	3.74	4.09	1.40	
C							2.39	3.81, 3.98
D	5.24		4.62	3.95	3.59	4.17	1.41	3.64
E	5.32	1.63	2.73	3.90	3.21	4.00		3.58
A′	4.20	3.32		4.32	2.39	3.90	1.37	
B′	5.16	1.87	2.24	4.29	3.74	4.09	1.40	
C′							2.39	3.81, 3.98
D′	5.24		4.62	3.95	3.59	4.17	1.41	3.64
E′	5.35	1.64	2.75	3.90	3.21	4.00		3.58

[a] The chemical shifts are referenced to 3-(trimethylsilyl)propionic-*2,2,3,3-d*$_4$ acid, sodium salt, using the HOD resonance previously calibrated in stock buffer solution. [b−h] Respectively interchangeable.

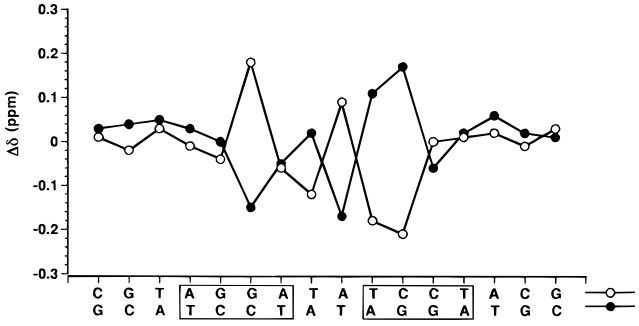

Figure 2. Chemical shift changes ($\delta_{free} - \delta_{bound}$) of the DNA H6/H8 protons (versus their location in the sequence) upon complexation with HHD (**3**).

The drug−DNA complex was prepared by dissolving known amounts of the ligand in MeOH, adding aliquots to 1 mL of a 1.0 mM solution of the duplex, and stirring at 25 °C for 5 min. After lyophilization, the complex was dissolved in 99.6% D_2O and the extent of the titration was determined by examining the DNA 6H/8H resonances in the ^{1}H NMR spectrum. The final solutions for NMR experiments were prepared in the same manner as for the free DNA duplex.

NMR Experiments. All NMR experiments were performed on a Bruker AMX-500 spectrometer. The NMR data were processed on a SGI INDIGO2 workstation using FELIX 2.3 software (Biosym, San Diego, CA). The temperature for all 2D experiments was 27 °C for both the free DNA duplex and the ligand−DNA complex. All spectra were acquired in the phase-sensitive mode with the transmitter set at the solvent resonance and TPPI (time proportional phase increment) used to achieve frequency discrimination in the ω_1 dimension.[17] The standard pulse sequence and phase cycling were used for two quantum spectroscopy (2Q)[18] and primitive exclusive correlation spectroscopy (PE-COSY)[19] spectra. A total of 48 scans/t_1 value were acquired for the 2Q (t_{mix} = 30 ms, t_{1max} = 50 ms) and the PE-COSY (t_{1max} = 80 ms) spectra. Total correlation spectroscopy (TOCSY) spectra were acquired using a DIPSI-2 sequence[20] for spin locking with t_{mix} = 70 ms, 64 scans/t_1 value and t_{1max} = 40 ms. Nuclear Overhauser effect spectroscopy (NOESY)[21] of H_2O solutions (t_{mix} = 200 ms, 64 scans/t_1, t_{1max} = 50 ms) was recorded with the last pulse replaced by a jump

(17) Marion, D.; Wüthrich, K. *Biochem. Biophys. Res. Commun.* **1983**, *113*, 500.
(18) Braunschweiler, L.; Bodenhausen, G.; Ernst, R. R. *Mol. Phys*. **1983**, *48*, 535.
(19) Mueller, L. *J. Magn. Reson.* **1987**, *72*, 191.
(20) Shaka, A. J.; Lee, C. J.; Pines, A. *J. Magn. Reson.* **1988**, *77*, 274.
(21) Macura, S.; Ernst, R. R. *Mol. Phys.* **1980**, *41*, 95.

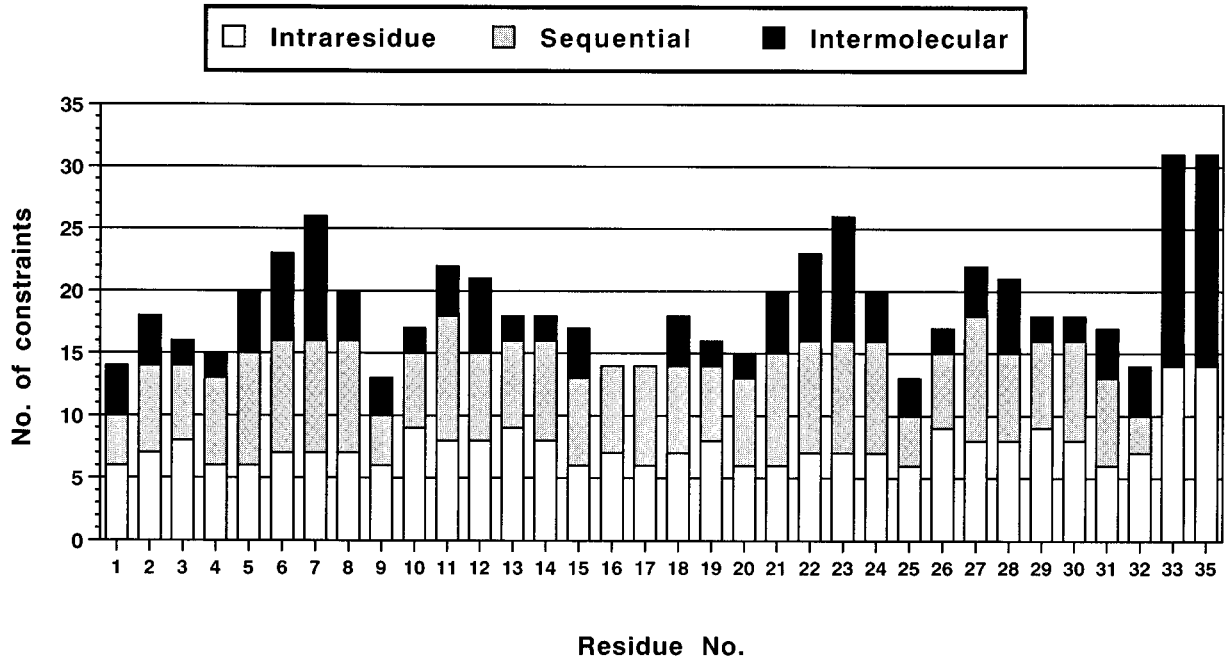

Figure 3. Plot of all the NMR-derived distance constraints used in the structure calculation of the HHD−DNA complex ordered by type.

and return composite sequence.[22] Two NOESY spectra (t_{mix} = 70 and 200 ms, 64 scans/t_1 and t_{1max} = 50 ms) from D_2O solution were recorded with saturation of the residual HOD resonance during the preparation and mixing periods and a Hahn-echo to improve the quality of the baseline.[23]

Structure Calculations. The structures of the complex were generated by a protocol involving several iterations through cycles of simulated annealing docking and refinement (Scheme 2). All restrained energy minimization (rEM) and restrained molecular dynamics (rMD) calculations were performed using the SANDER module of AMBER 4.1[24] on a Convex C-240 Meta-Series Supercomputer. The potential functions for distance and dihedral constraints were flat between the given upper and lower bounds and rose parabolically outside of these bounds. Using a special feature of SANDER, the parabolic function was smoothly converted into a linear function, in order to avoid large violations. No explicit solvent molecules were included in these calculations, so a distance dependent dielectric and reduced net charges on the phosphate oxygens (−0.2) were used to partially compensate for the absence of solvent. A distance cutoff of 9 Å was set for all nonbonded interactions. The force constant for both distance and dihedral constraints was 32 kcal/mol Å^2.

The simulated annealing docking procedure involved placing the oligosaccharide and DNA molecules *ca*. 20 Å apart on a course grid using the program Nucleic Acid Builder (NAB).[25] The initial conformation of the head-to-head calicheamicin oligosaccharide dimer was generated in Insight II by bonding two oligosaccharide molecules (derived from our structural model of the calicheamicin−DNA complex)[9] to a bis(ethylene glycol) linker followed by energy minimization. Fourteen different right-handed helical DNA starting conformations were generated using NAB. The root mean square deviation (RMSD) between these fourteen structures is 6.5 Å. The alignment between the oligosaccharide molecule and each DNA conformation was made using six pairs of atoms, with one each from the DNA and the ligand selected on the basis of high likelihood of their involvement in direct intermolecular contacts. After alignment, 30 ps of rMD simulated annealing to 1000 K was performed with very slow ramping up of the force constant for the experimental intermolecular constraints (0.1−32 kcal/mol Å^2). These docked structures were refined by an additional 20 ps of rMD simulated annealing to 1000 K. The structures were then arranged in order of experimental constraint violation energy and the best seven were selected to represent the ensemble.

Table 2. HHD−DNA Intermolecular NOEs Observed for the 1:1 Complex d(CGTAGGATATCCTACG)$_2$−HHD Measured at 300 K

proton 1 (HHD, 3)	proton 2 (DNA)	size[a]	proton 1 (HHD, **3**)	proton 2 (DNA)	size[a]
B-Me	C_{12}-4′H′	s	B′-Me	C_{28}-4′H′	s
B-H1	T_{24}-4′H′	s	B′-H1	T_8-4′H′	s
B-H1	T_{24}-H5′	s	B′-H1	T_8-H5′	s
B-H2$_{ax}$	A_{23}-2H	m	B′-H2$_{ax}$	A_7-2H	m
B-H2$_{eq}$	A_{23}-2H	m	B′-H2$_{eq}$	A_7-2H	m
B-H2$_{eq}$	G_{22}-1H	w	B′-H2$_{eq}$	G_6-1H	w
B-H3	A_{23}-2H	s	B′-H3	A_7-2H	s
B-H3	G_{22}-1H	w	B′-H3	G_6-1H	w
D-H1	A_{23}-5′H	s	D′-H1	A_7-5′H	s
D-H1	A_{23}-5″H	s	D′-H1	A_7-5″H	s
D-H2	A_{23}-5′H	s	D′-H2	A_7-5′H	s
D-H2	A_{23}-5″H	s	D′-H2	A_7-5″H	s
D-Ome	G_{22}-4′H	m	D′-Ome	G_6-4′H	m
D-Ome	G_{21}-2H	w	D′-Ome	G_5-2H	w

[a] w = weak, m = medium, s = strong. This categorization is based on the volume of the NOESY cross peaks (τ_{mix} = 70 and 200 ms).

Results and Discussion

The general strategies for sequence-specific assignment of the ^{1}H resonances of small DNA duplexes have been amply reviewed,[26] and the specific protocols used here for the free DNA and the ligand−DNA complexes have been described.[5,9] The shorthand notation described by Wüthrich[26b] is used to specify DNA interproton distances and corresponding nuclear Overhauser effects NOEs.

^{1}H NMR of the Free Duplex. All cytosine 5H−6H and thymine 5Me−6H resonances were readily identified by scalar connectivities in 2Q, PE-COSY and TOCSY spectra. All 32 1′H−2′H−2″H−3′H spin subsystems could be identified in the 2Q, PE-COSY, and TOCSY spectra and were confirmed by inspection of the NOESY spectra. The sequential resonance assignments were made in the 70 ms mixing time NOESY spectrum. The combination of d_i(6,8;2′), d_s(2″;6,8), d_i(5Me;6),

(22) Plateau, P.; Guéron, M. J. *J. Am. Chem. Soc*. **1982**, *104*, 7310.
(23) (a) Davis, D. G. *J. Magn. Reson.* **1989**, *81*, 603. (b) Rance, M. Byrd, R. A. *J. Magn. Reson*. **1983**, *54*, 221.
(24) Pearlman, D. A.; Case, D. A.; Caldwell, C. J.; Seibel, G. L.; Singh, U. C.; Weiner, P.; Kollman, P. A. AMBER 4.0 1991; University of California: San Francisco. Pearlman, D. A.; Case, D. A.; Yip, P. AMBER 4.0 1991; University of California, San Francisco.
(25) Macke, T. doctoral thesis, The Scripps Research Institute, 1996.
(26) (a) Wemmer, D. E.; Reid, B. R. *Annu. Rev. Phys. Chem.* **1985**, *36*, 105. (b) Wüthrich, K. In *NMR of Proteins and Nucleic Acids*; Wiley: New York, 1986. (c) Patel, D. J.; Shapiro, L.; Hare, D. *Annu. Rev. Biophys. Chem.* **1987**, *16*, 423. (d) Reid, B. R. *Q. Rev. Biophys*. **1987**, *20*, 1.

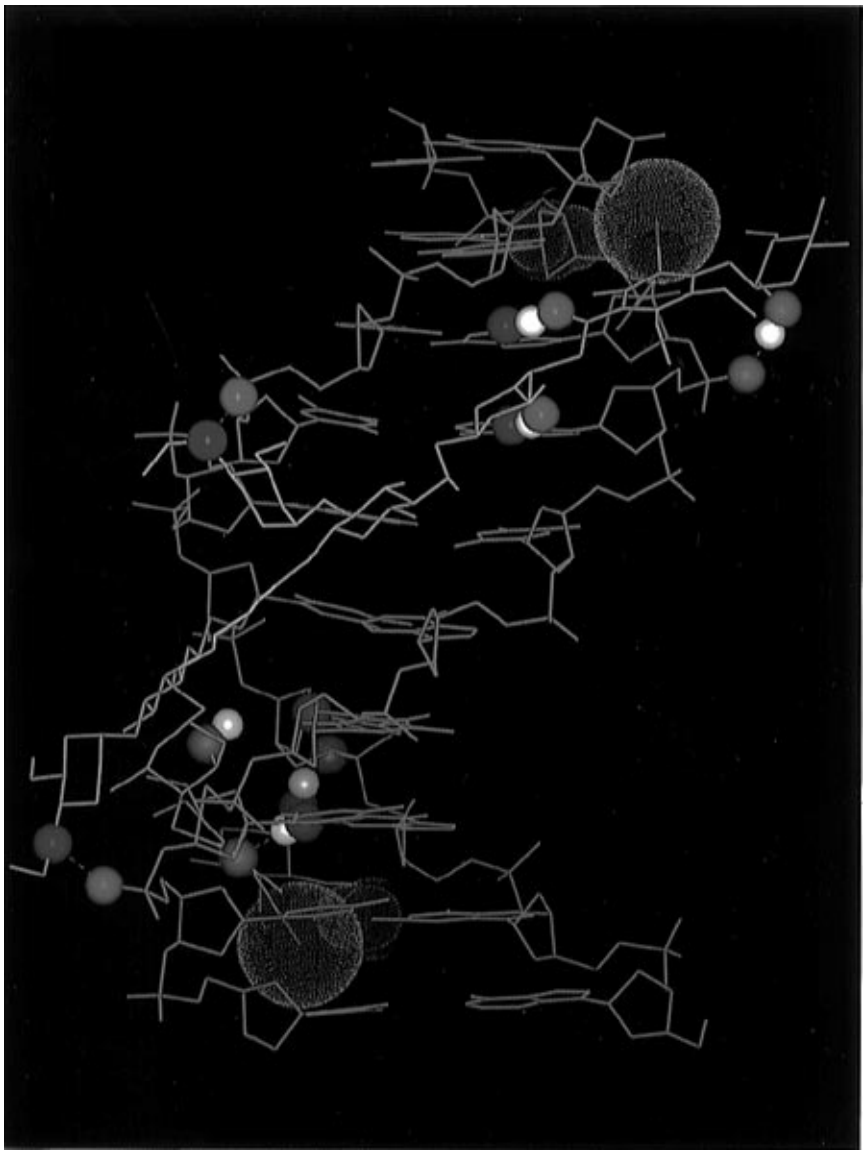

Figure 4. Wireframe model of the HDD-DNA complex showing the gentle curvature of the HHD molecule (oligosaccharide units in yellow, linker in white) that follows the helical geometry of the DNA (green).

d_s(6,8;5Me) were sufficient to obtain complete sequence-specific resonance assignments (Table S1 of the supporting information). The relative intensities of NOESY cross peaks [*e.g.*, d_i(6,8;2′), d_s(2″;6,8) ≫ d_i(6,8;2″), d_s(2′;6,8) and d_i(5Me;6) > d_s(6,8;5Me)] and the cross peak patterns in the PE-COSY spectrum clearly indicated that d(CGTAGGATATCCTACG)$_2$ is a B-form duplex with predominantly C_2'-*endo* sugar conformations.

Characterization and ^{1}H NMR Assignments of the HHD 3−DNA Complex. Upon binding of the head-to-head dimer to the DNA, an increase in the line widths of all DNA and saccharide resonances was observed. The C_2 symmetry of the duplex was clearly broken, giving rise to nearly two times the number of NMR signals. Variable temperature 1D ^{1}H-NMR studies were performed in an attempt to analyze the dynamic behavior of the complex. Indepth analysis of the 2Q, TOCSY, and NOESY experiments provided the critical sequence-specific ^{1}H assignments for both strands, which are listed in Table 1. The relative intensities of cross peaks in the 70 ms NOESY indicated that the duplex remains within the B-form structural family with a predominance of $C_{2'}$-*endo* sugar conformations.

DNA and HHD 3 Complexation Shifts. The change in chemical shifts of selected DNA protons induced by the binding of the ligand ($\Delta\delta_{\text{free−bound}}$) are plotted in Figure 2. These data identify the ligand binding site and any additional perturbations of the DNA in adjacent base pairs. Significant chemical shift differences in the resonances of DNA base protons facing the minor groove were observed in both binding sites, particularly at the G_6/C_{27}, T_{10}/A_{23}, and C_{11}/G_{22} base pairs, consistent with a bidentate mode of binding of the oligosaccharide dimer. The two binding sites apparent from this analysis are $A_4/T_{29}-A_7/T_{26}$ and $A_{20}/T_{13}-A_{23}/T_{10}$. Interestingly, significant differences in chemical shifts extend outside the binding site to the two terminal regions of the DNA duplex. These are presumably due to structural pertubations induced by ligand binding. It is remarkable that the chemical shift changes detected outside the direct region of binding in the calicheamicin (**1**) complex, are both qualitatively and quantitatively reproduced in the complex of HHD **3**. This provides strong evidence that the binding mode of both units of the dimer to the DNA is the same as that observed in the corresponding complexes of the oligosaccharide monomer and intact calicheamicin.

NMR-Derived Distance and Torsion Constraints. Analysis of the three NOESY spectra provided 342 DNA−DNA, 28 oligosaccharide−oligosaccharide, and 34 oligosaccharide−DNA distance restraints. The distribution of these restraints is shown in Figure 3. An additional 48 additional distance restraints were included on the basis of the Watson−Crick hydrogen bonds indicated by the characteristic chemical shifts of the imino and

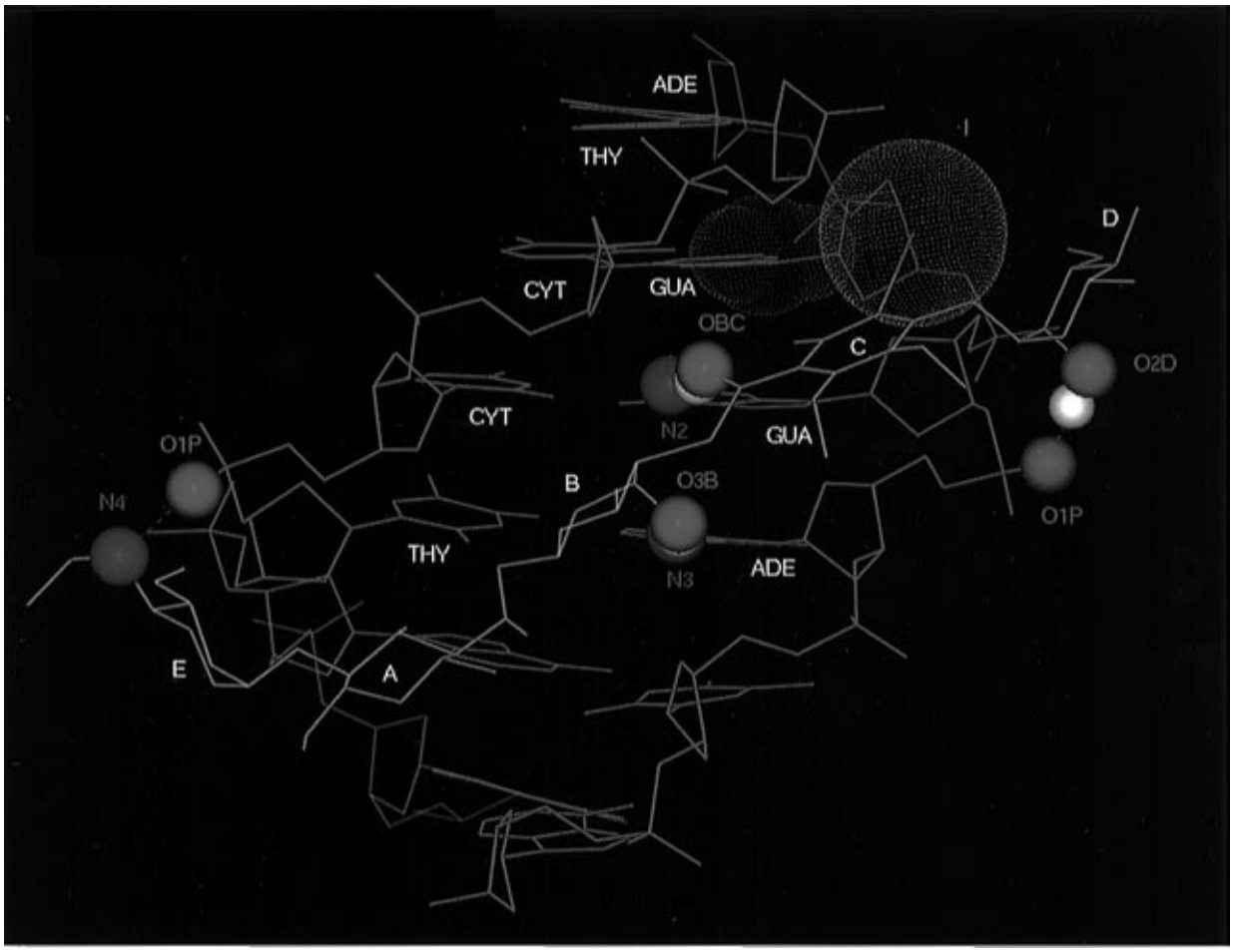

Figure 5. Expanded region of a wireframe model of the HDD−DNA complex showing the major intermolecular interactions between one of the two oligosaccharide units (yellow) and the corresponding DNA residues (green) within the recognition site.

cystosine amino protons. The NOE-derived distance restraints were refined by relaxation matrix analysis using the program MARDIGRAS 5.1,[27] for all accurately measured cross peak intensities in all three NOESY spectra. A reference model was constructed in Insight II by manually docking a model-built structure of the oligosaccharide dimer into the minor groove of a model of the duplex in standard B−DNA geometry. An additional 10% of the target distance was added to the MARDIGRAS upper bound to account for experimental uncertainties.

The values of $J_{1'-2'}$ and $J_{1'-2''}$ scalar coupling constants (plus an estimate for the magnitude of $J_{2'-3'}$ and $J_{2''-3'}$) were obtained from analysis of PE-COSY cross-peaks. These coupling constants were converted into a pseudorotation phase angle (PPA) by standard methods and applied as deoxyribose ring torsion angle constraints on the angles ν_0, ν_1, ν_2, ν_3, and ν_4. The PPA angles ranged between 90° and 190° (PPA for standard B DNA is *ca.* 160° and for A−DNA *ca.* 20°). Restraints for the DNA backbone torsions γ and ϵ were derived by the method of Reid and co-workers.[28] Limits on the sum of all scalar couplings to H-4′ and H-3′ were estimated from ω_2 cross sections of isolated NOESY crosspeaks. Constraints on both γ and ϵ were obtained for all DNA residues. Typical values were in the ranges 20°−100° for γ and 240°−300° for ϵ. In all, 155 torsion angle restraints were identified.

Solution Structure of the HHD−DNA Complex. The protocol used for the structure calculations of the HHD−DNA complex is summarized in Scheme 2. Our methodology for structure determination of ligand−DNA complexes is discussed in detail elsewhere (J. Smith, L. Gomez-Paloma, D. A. Case, W. J. Chazin, *Magn. Reson. Chem.*, submitted). As noted above, direct evidence for the binding of the oligosaccharide **3** to DNA is provided by a number of NOESY intermolecular peaks and by the $\Delta\delta_{\text{free-bound}}$ induced by the saccharide upon complexation (Figure 2). The HHD−DNA intermolecular NOESY cross peaks unambiguously assigned are listed in Table 2. The full list of proton−proton distances derived from the NOESY spectra used in the structure calculations is provided as supporting information (Table S2). The pattern of intermolecular NOESY peaks is remarkably similar to that already observed in the calicheamicin−DNA complex, strongly indicating that the binding mode of the aryltetrasaccharide moiety is the same in both cases. An overview of the structure of the complex is provided in Figure 4. All of the carbohydrate residues except rings E and E′ are found to make direct contact with the DNA. The proton signals of the bis-(ethylene glycol) linker could not be assigned due to severe resonance overlap among themselves and with the H4′ and H5′/H5″ DNA signals. Since no intermolecular contacts could be identified, these atoms are ordered only indirectly, as a result of their linkage to the two bound oligosaccharide domains.

The wireframe model of the HDD−DNA complex displayed in Figure 5 clearly shows the gentle curvature of the HHD molecule following the helical geometry of the DNA. This property allows close contact and a large area of interaction between the two molecules along all of the HHD residues except rings E and E′. The HHD−DNA complex appears to be stabilized by a number of intermolecular interactions, as previously observed for the calicheamicin−DNA complex. All of the *major* interactions between each oligosaccharide unit of HHD and the corresponding DNA residues within the recogni-

(27) Borgias, B. A.; James, T. L. *J. Magn. Reson.* **1990**, *87*, 475.
(28) Kim, S. G.; Lin, L. J.; Reid, B. R. *Biochemistry* **1992**, *31*, 3564.

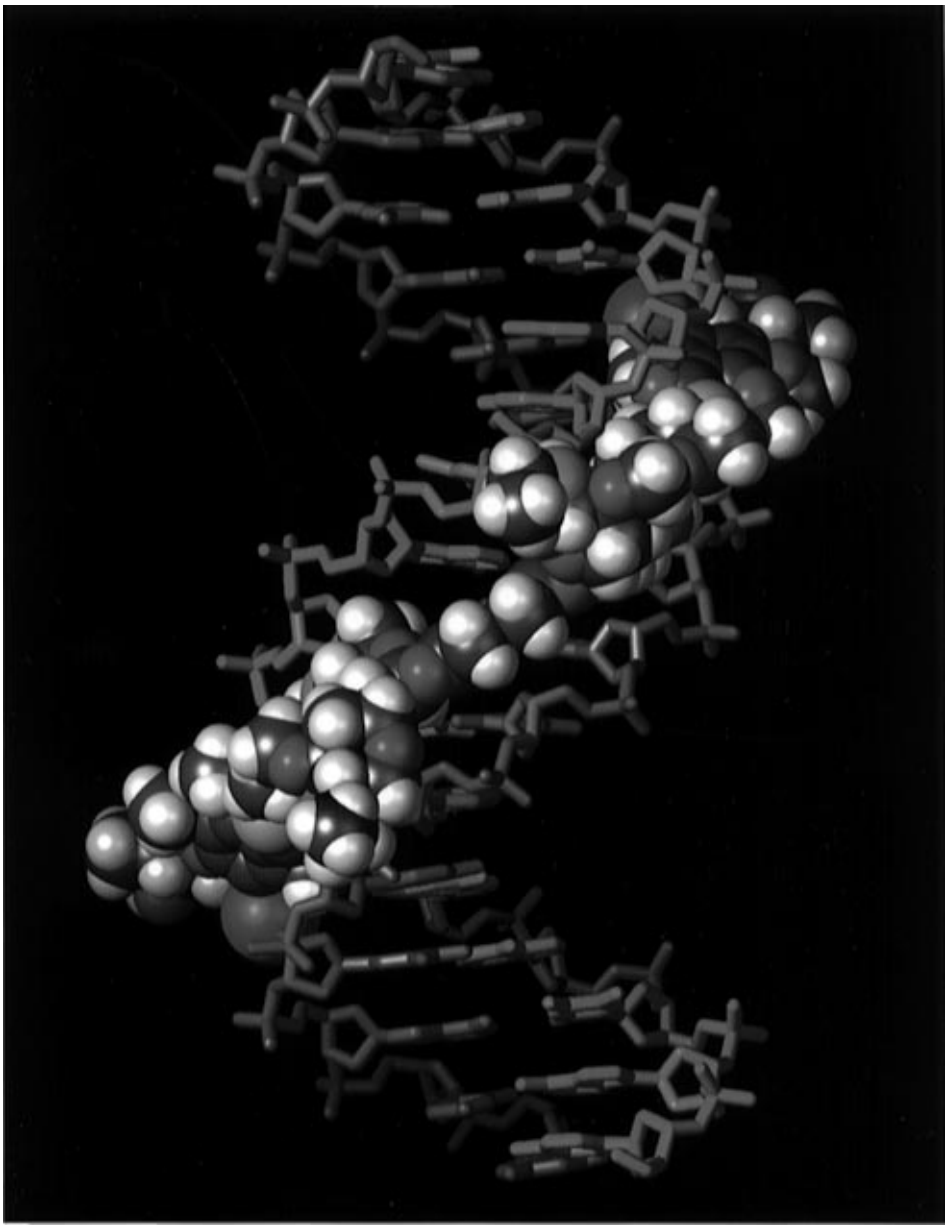

Figure 6. CPK model of the HHD in the HHD−DNA complex. The DNA strands are displayed in red and green. The HHD atoms are displayed in different colors according to the atom type (carbon, gray; hydrogen, white; nitrogen, blue; oxygen, red; sulfur, yellow; and iodine, magenta).

tion site are represented in Figure 6. Van der Waals interactions must contribute significantly to the binding as a byproduct of the lypophilic nature of the aryltetrasaccharide and the hydrophobic character of the DNA minor groove. The aromatic rings C and C′ show stacking interactions with the deoxyribose ether oxygens O4′ of A_7 and A_{23}, respectively. Electrostatic contacts also play an important role in the binding, as demonstrated by the presence of two equivalent salt bridges between the positively charged nitrogens of rings E and E′ and the negatively charged backbone oxygens C11−O1′ and C27−O1′, respectively. The unusual contact (∼4.0 Å) between the iodine atom attached to the C ring and a guanine amino group, previously noted in the calicheamicin−DNA complex, both in structural models[9,29] and by kinetic studies,[30] is faithfully reproduced in the HHD−DNA complex in both recognition sites. A listing of the donor and acceptor atoms involved in the formation of the eight intermolecular H-bonds is reported in Table 3.

In the complex, all of the HHD residues are located in well-defined positions, except rings E and E′. Indeed, intermolecular NOESY cross peaks from rings E and E′ to DNA residues could not be observed under our experimental conditions, in agreement with the fact that these residues lie outside of the minor groove (see also the calicheamicin−DNA complex)[9,29] and suggesting that they are characterized by a higher degree of conformational flexibility.

Table 3. HHD−DNA Intermolecular H Bonds[a] Observed in the Solution Structure for the 1:1 HHD−DNA Complex

donor	acceptor	donor	acceptor
B-3O*H*	A_{23}-*N*3	B′-3O*H*	A_7-*N*3
G_{22}-N*H*2	C-SC=*O*	G_6-N*H*2	C′-SC=O
D-2O*H*	A_{23}-*O*1P	D′-2O*H*	A_7-*O*1P

[a] The H-bonds are defined by a distance cutoff of 3.0 Å.

Dynamics of the HHD−DNA Complex. As noted above, the HHD−DNA complex exists as a mixture of two equally populated, structurally similar conformational substates, slowly interconverting with respect to the NMR time scale. Since the two substates give rise to NMR peaks with equal intensity, we can conclude that these two states must have the same potential energy. This is also confirmed by the observation that the ratio between the peaks assigned to the two different substates does

(29) Norihiro, I.; Ajay Kumar, R.; Ling, T.-T.; Ellestad, G. A.; Danishefsky, S. J.; Patel, D. J. *Proc. Natl. Acad. Sci., U.S.A.* **1995**, *92*, 10506.
(30) Li, T.; Zeng, Z.; Estevez, V. A.; Baldenius, K. U.; Nicolaou, K. C.; Joyce, G. F. *J. Am. Chem. Soc*. **1994**, *116*, 37089.

Scheme 3. Model Proposed to Explain the Exchange Phenomenon Observed in the Spectra of the HHD−DNA Complex[a]

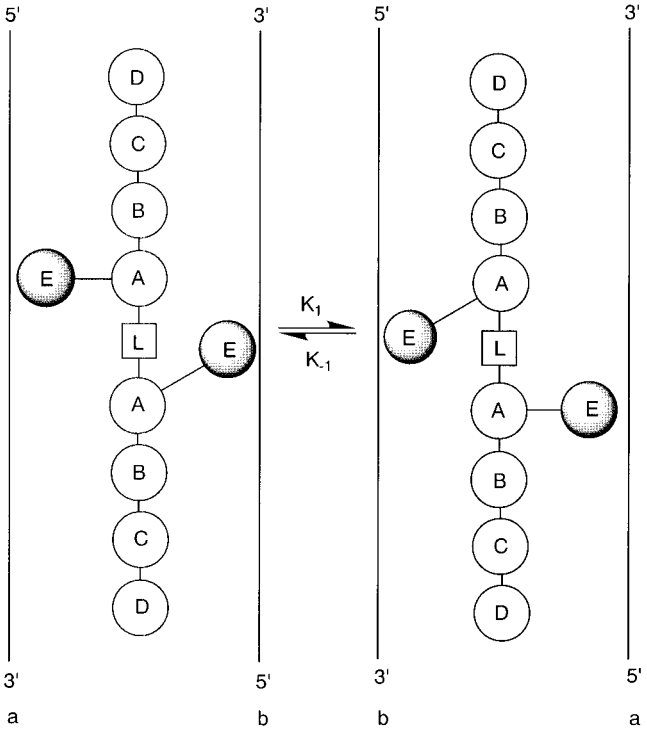

[a] The slow interconversion among the two equally populated substates could be caused by an alternative repositioning of rings E and E′, as displayed.

not change under a wide range of temperatures and conditions (0−47 °C). We propose that this equilibrium corresponds to alternate positioning of rings E and E′, for example, as displayed in Scheme 3. This model is supported by the largest chemical shift differences between the two states occurring exactly for the DNA residues closest to the linker and the E and E′ rings (e.g. T_8, A_9, T_{24}, A_{25} residues). In this scenario, the two strands of the DNA palindrome become nonequivalent upon complexation to HHD, but they interconvert. Since it has not been possible to observe coalescence of any of the pairs peaks related by the exchange process, the $\Delta G^{\ddagger}$ activation energy for the phenomenon could not be calculated. However, the rate constant for the exchange[31] between the two substates of the HHD−DNA complex at 300 K was estimated as 0.35 s^{-1}, on the basis of the ratio of cross peak volumes to diagonal volumes[32] for several exchanging DNA resonances in the NOESY spectra (Figure 7).

Conclusion

The tethered head-to-head dimer of the calicheamicin oligosaccharide domain was designed to generate a higher level of binding affinity and sequence specificity than the oligosaccharide monomer. A bis(ethylene glycol) linker was used to connect the two monomers so that the tether would possess sufficient flexibility to allow each domain to adapt to its specific binding site. Inspection of the solution structure of the head-to-head dimer−DNA complex indicates that the binding mode of each carbohydrate unit of the dimer **3** in the minor groove is very close to that observed in the case of the monomeric carbohydrate **2** bound to a TCCT DNA site. Indeed all the ligand−DNA interactions observed in the monomeric oligosaccharide−DNA complex are faithfully reproduced in the present head-to-head dimer−DNA complex. Thus, the design objectives for the dimeric system have been met. The structural data from the present study together with the increased selectivity, nanomolar affinity, and the interesting biological activity[16] of the dimeric oligosaccharide **3** strongly suggest that carbohydrates can be used as a means for generating DNA target specificity and may enable the control of the function of nucleic acids.

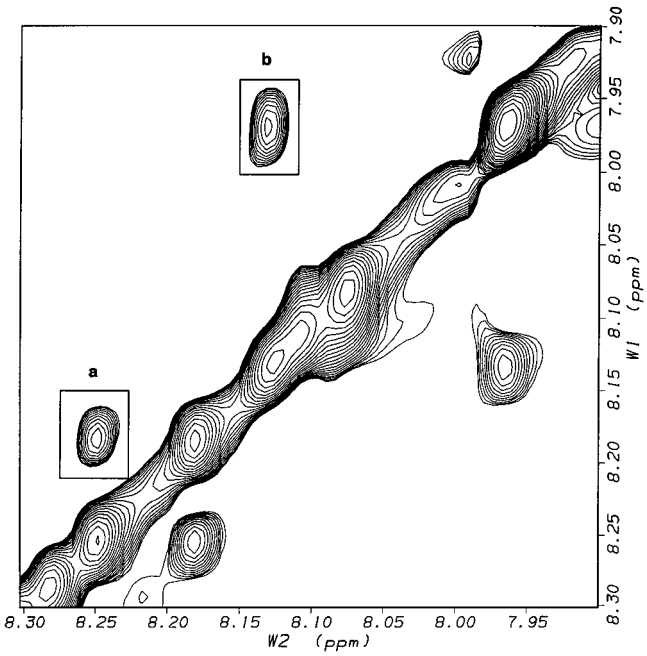

Figure 7. Expanded region of the 500-MHz NOESY spectrum (τ_m = 200 ms, T = 300 K) of the HHD−DNA complex. The cross peaks in the boxes arise from chemical exchange between the two interstates: (a) A_9/A_{25}-8H; (b) A_7/A_{23}-8H.

Acknowledgment. This paper is dedicated to Nelson Leonard on the occasion of his 80th birthday. We thank Prof. L. Mayol for providing us with the DNA oligomers used in this study. L.G.P. is a visiting Assistant Professor on leave from University of Naples "Federico II". Financial assistance was provided by the National Institutes of Health (U.S.A.) and by The Scripps Research Institute (to K.C.N.). W.J.C. is supported by grants from the American Cancer Society (DHP-123, FRA-436).

Supporting Information Available: Listings of proton chemical shift assignments of the free DNA (Table S1), NMR-derived experimental constraints used in the structure calculation (Table S2) and expanded regions of NOESY spectra of the HHD−DNA complex (Figures S1, S2, and S3) (13 pages). See any current masthead page for ordering and Internet access instructions.

JA961525N

(31) Sandström, J. *Dynamic NMR Spectroscopy;* Academic Press: New York, 1982.

(32) Jeener J.; Meier, B. H.; Bachmann, P.; Ernst, R. R. *J. Chem. Phys.* **1979**, *71(11)*, 4546.